CHAPTER 6

AUTOMATIC POLARIZATION CONTROL EXPERIMENTS UTILIZING POLARIZATION RECOMBINING SCHEME

6.1. Introdution

In this chapter, polarization-state control experiments utlizing polarization recombining schemes (Type-I and Type-II) are presented. The principle of the SOP control for these schemes is very simple and endlessness (resetting-free) in control is achieved. As compared with previous SOP control schemes [80-90], in the present schemes linear SOP of the ouput light with a fixed inclination angle (or deflection) angle indepentdent of the incoming SOP is always maintained without the aid of a polarimeter, whereas in the formers a bulk optical polarimeter system is required in order to obtain or maintain linear SOP of the signal light at the receiving end. Such a characteristic of the polarization recombining scheme is particularly useful in a phase-diversity homodyne receiver because a stable linearly polarized signal light is necessary for generating an in-phase and a quadrature IF signal [27]. An automatic polarization-state control experiment on 200 Mbits/s DPSK self-homodyne phase diversity receiver utlizing the Type-II polarization recombining scheme is also demonstrated.

6.2. Type-I polarization recombining scheme

6.2.1. Principle

The schematic diagram of the proposed SOP control scheme is shown in Fig. 46 together with its experimental setup. The scheme itself is shown enclosed by a dotted line, and consists of a polarization beam splitter (a Wollaston prism), a 90° linear polarization rotator (hereafter 90°-LPR, for short), an endless phase shifter, a half mirror, and two photodetectors followed by signal processing electronics. The principle of the scheme is as follows. Signal light after propagating through a long single-mode fiber arrives at the fiber exit in an arbitrary SOP, is separated into two orthogonal linearly polarized components (i.e. H: and V: components) by the Wollaston prism. The V: component is converted into a H: component by rotating its polarization plane by 90° using a 90°-LPR, and then recombined with the other H: component in the half mirror. When the phase difference between the two arms of the interferometer is $m\pi/2$ ($m = \pm 1, \pm 3, \pm 5, \ldots$), the output intensities at ports 1 and 2 will be equal regardless of the different relative intensities in the two arms. The SOP's of the two ouput lights are the same and always linear with a fixed inclination angle determined by the principal axis of the Wollaston prism independent of changes in the SOP of the input signal light. In this scheme, therefore, the phase shift given by the

endless phase shifter is adjusted so that the output intensities at ports 1 and 2 detected by the photodetectors P1 and P2, respectively, are equal.

After this work had almost been completed, an equivalent scheme based on the same principle was reported by Mahon and Khoe [93]. In their scheme (see Fig. 47), the SOP of the received signal is controlled by using two fiber squeezers placed before the polarization beam splitter. These elements squeeze the fiber at 0° and 45° with respect to the fiber fast axis. The ellipticity is thus contolled so that the required 90° phase shift between the two arms of the interferometer is achieved. However, due to the finite control range of the devices, reset is necessary to maintain endless operation. On the other hand, the present scheme proposed here allows resetting-free operation.

6.2.2. Experiment and results

The experimental setup which is sufficient for demonstrating the principle of the scheme, is also shown in Fig. 46. The output of a 1.35 μm DFB semiconductor laser was linearly polarized and launched into a 1.5-km-long single-mode fiber (SMF) by using a polarizer and a HWP. At the fiber exit, a Babinet-Soleil compensator (BSC) was used to disturb the SOP of the received light. The 45°-oriented Wollaston prism splitted the light into two orthogonal linearly polarized lights, a 45°-inclined linearly polarized

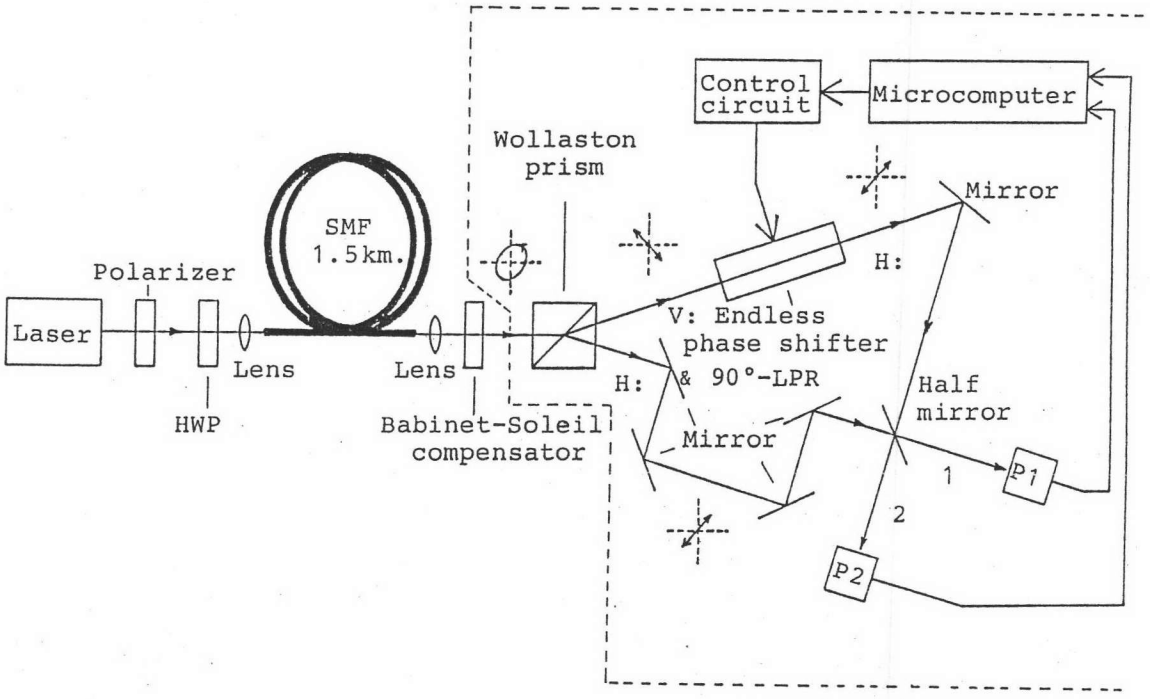

Fig. 46. Experimental setup of polarization-state control system utilizing Type-I polarization recombining scheme.

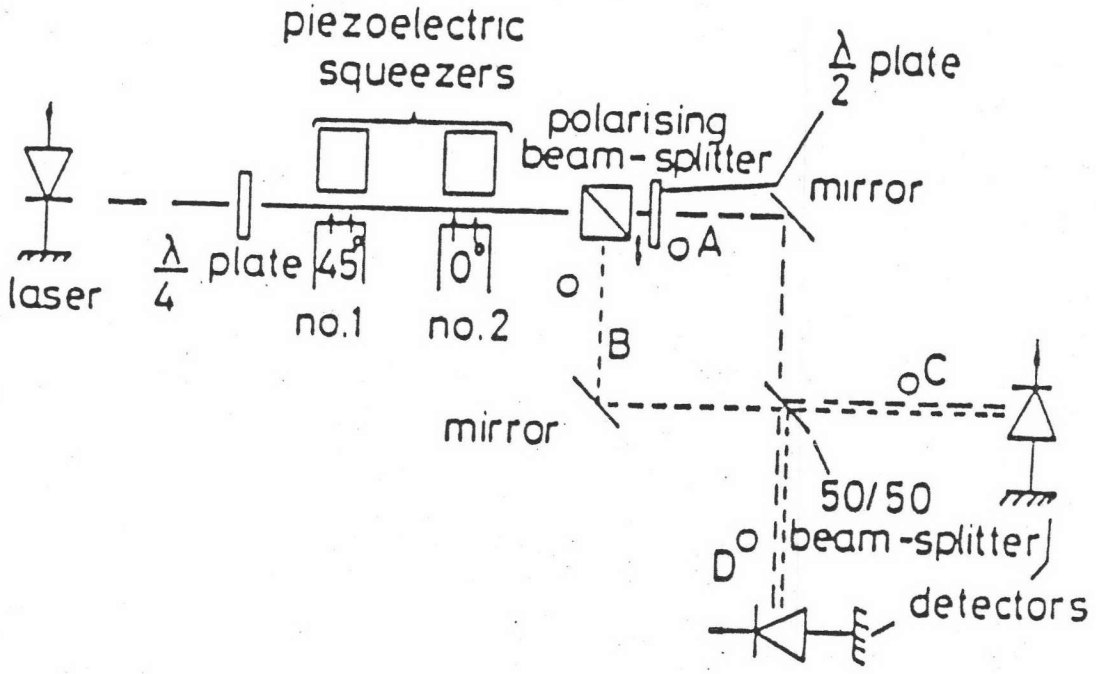

Fig. 47. Experimental setup of polarization-state control system equivalent to the Type-I polarization recombining scheme (after Makon and Khol [93]).

light and a -45°-inclined linearly polarized light. The endless phase shifter (see Fig. 37) was inserted in the arm of the -45°-inclined linearly polarized light and also used as a 90°-LPR. The ouput intensities at ports 1 and 2 were detected by the Ge-APD photodetectors P1 and P2, respectively.

To demonstrate the scheme, the SOP of the input light to the polarization controller was intentionally disturbed by manipulating the BSC and by heating a short length of the fiber by using a hair dryer, and the variations of the photodetector currents P1 and P2 were observed. The SOP was controlled through a microcomputer in the following way. The rotatable HWP (hereafter RHWP) of the endless phase shifter was rotated by a stepping motor (1.8/step) driven by a stepping pulse (4 Hz). First, a stepping pulse rotates the RHWP by one step. If $|P1-P2|$ decreases, the next pulse rotates the RHWP in the same direction. If $|P1-P2|$ increases, the next pulse rotates the RHWP in the opposite direction. This process is repeated until the optimum condition P1=P2 is achieved.

An example of the experimental results is shown in Fig. 48. It is found in Fig. 48(a) that the variations of P1 and P2 are kept within + 2.5% when the SOP of the light has been drastically disturbed (indicated by the arrows) and are kept less than + 1% during the disturbance-free condition under automatic polarization con-

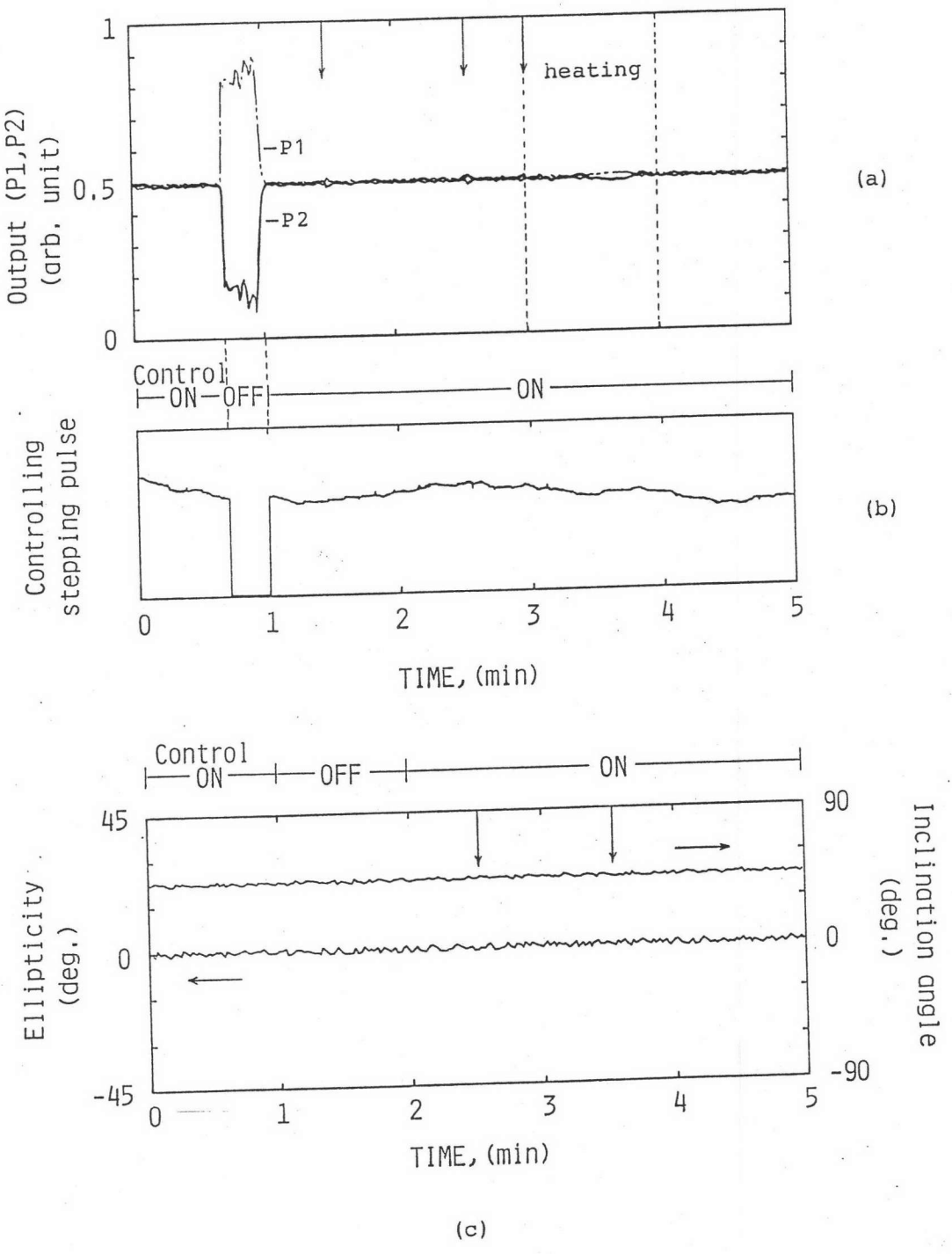

Fig. 48. Results of the polarization-state control experiment utilizing Type-I polarization recombining scheme. The vertical arrows indicate the times when the SOP of the light in the fiber was desturbed.

trol. Figure 48(b) shows the variations of the controlling stepping pulse. Figure 48(c) shows the polarization characteristics of the output light which has been measured by using a polarimeter located in place of the photodetector P2. As expected, the SOP of the output light is always linear with a fixed inclination angle (45° in this case) regardless of changes in the SOP of the input light (indicated by the vertical arrows) with and without automatic polarization control. In this measurement, only the BSC was used to disturb the SOP of the input light. Ripples in the resulting curves are mainly due to mechanical, laser intensity fluctuations and other instabilities.

6.2.3. Discussion

In an actual coherent communication system utilizing the proposed SOP control scheme, the intermediate frequency (IF) signals are used for the automatic feedback optical phase control. Schematic diagram of an optical coherent communication system incorporating the present SOP control scheme is illustrated in Fig. 49. This system is similar to the polarization diversity receiver recently suggested by Okoshi and Ryu [29]. The differences are that ,in the present system, the phase compensation is done in the optical frequency domain with much simpler control procedure, rather than in the intermediate frequency (IF) domain, and the adjustment of the inclination angle of the received signal light

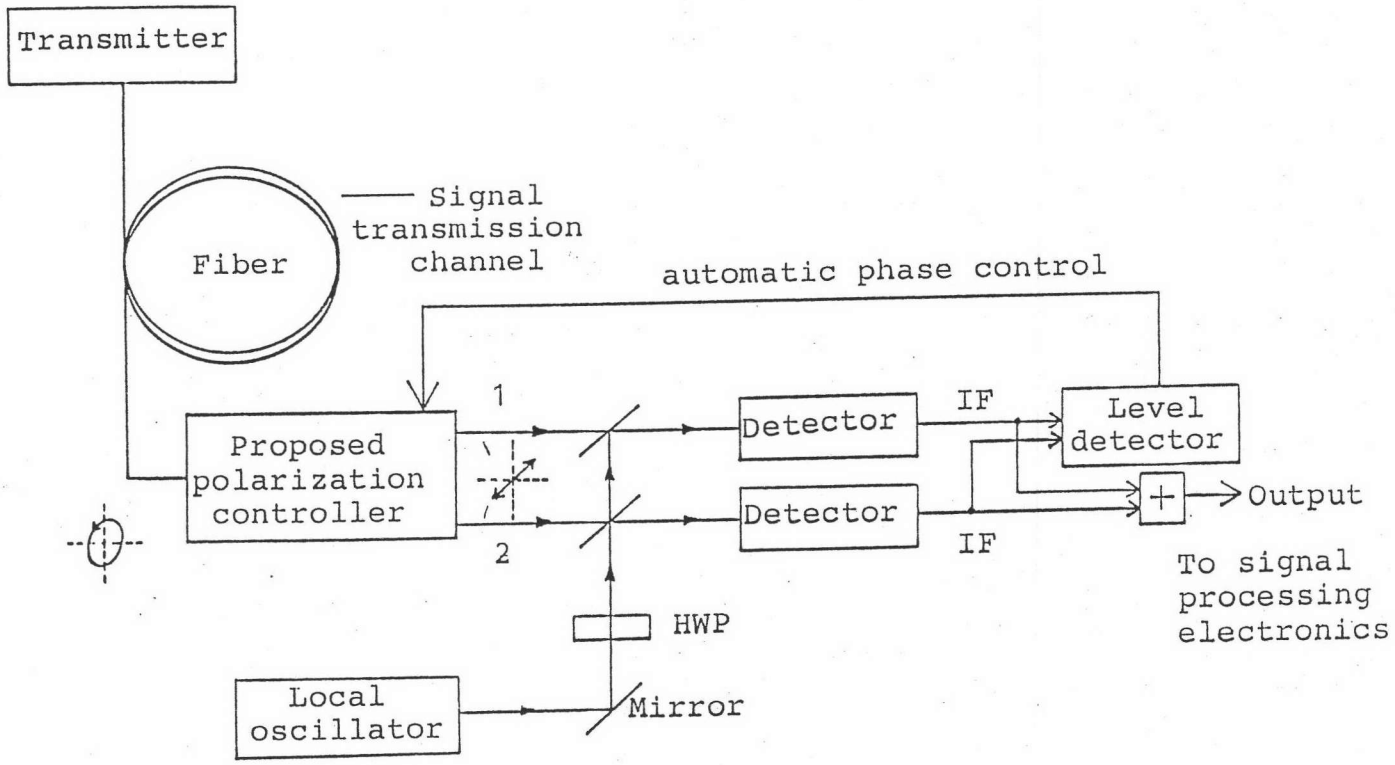

Fig. 49. System configuration of an endless SOP control utilizing Type-I polarization recombining scheme for coherent (heterodyne or homodyne) optical receiver.

is not needed. This reduces an overall complexity of the signal processing electronics.

6.3. Type-II polarization recombining scheme

6.3.1. Principle

The schematic diagram of this type together with its experimental set-up is shown in Fig. 50. The principle of operation is similar to that of Type-I. The difference is that in this type one of the two branches is used for signal detection, and another is used for polarization-state monitoring. When the phase difference between the two arms of the interferometer is $2m\pi$ (m:interger) and the magnitudes of the H: and V: components are equal the maximum interfering output can be obtained at branch 1 and is used for signal detection. In this scheme, therefore, the polarization inclination angle given to the signal light by the polarization rotator (FC2) and the phase shift given by the endless phase shifter are adjusted so that the output to the monitor branch 2 is minimized.

6.3.2. Experiment and results

Figure 50 shows the experimental set-up used to demonstrate the proposed polarizaton control scheme. Light from a 1.35 μm DFB laser was linearly polarized and launched into a 1.5-km-long single-mode optical fiber by using a linear polarizer and the Babinet-

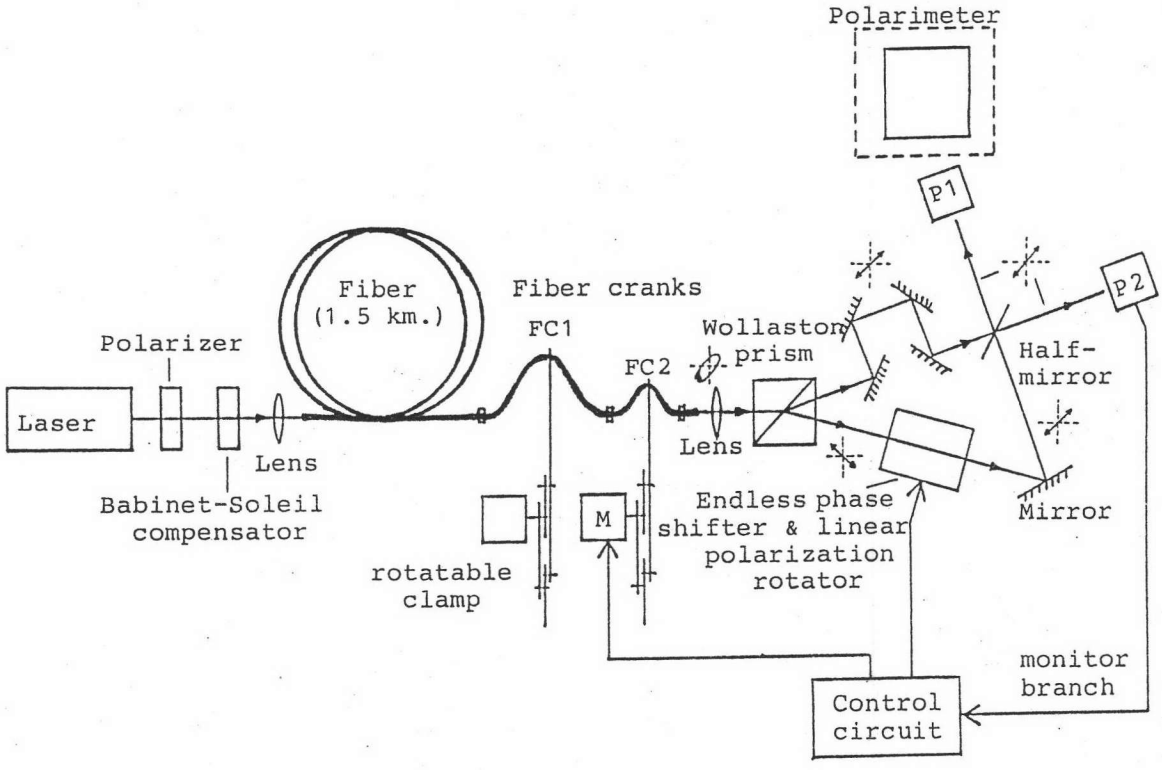

Fig. 50. Experimental setup of polarization-state control system utilizing Type-II polarization recombining scheme.

Soliel compensator (BSC) which used as a HWP. The QWP-equivalent fiber crank FC1 was used to produce arbitrary elliptically polarized light in the fiber and the rotatable HWP-equivalent fiber crank FC2 was used as the polarization rotator. The 45°-oriented Wollaston prism splitted the incoming light into two orthogonal linearly polarized lights: a 45°-inclined and a -45°-inclined linear polarizations. The Type-II endless phase shifter described in Chapter 5 was inserted in the -45°-inclined linear polarization arm and also used as a 90° linear polarization rotator.

Stepping motors were used to rotate the FC2 and the rotatble HWP in the phase shifter. The control procedure was proceeded in the following manner through a microprocessor. First, a stepping pulse (4Hz) rotates the FC2 by one step (1.8°). If the direct-detected output P2 decreases, the next pulse rotates the FC2 in the same direction. (If P2 increased in the opposite direction.) This " minimum-search " process is repeated ten times each for the FC2 and the rotatable HWP alternately, so that P2 is always minimized.

To demonstrate the scheme, the FC1 was manually rotated in order to disturb the SOP of light in the fiber, and variations of the photodetectors' currents P1 and P2 were automatically recorded. An example of the results is shown in Fig. 51. It is found that P2 increases once by 4 dB but returns to its minimum value

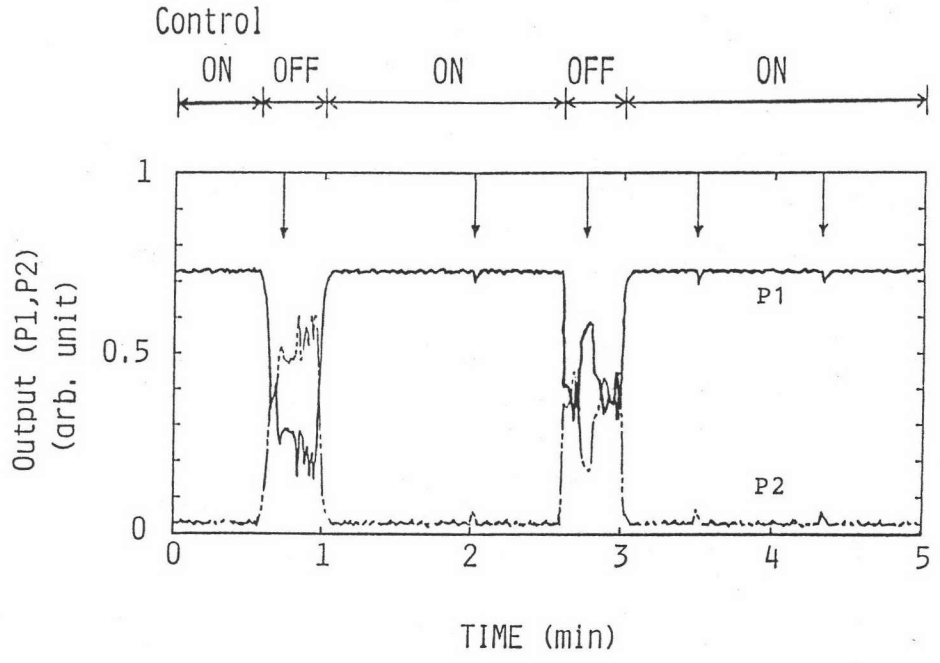

(a)

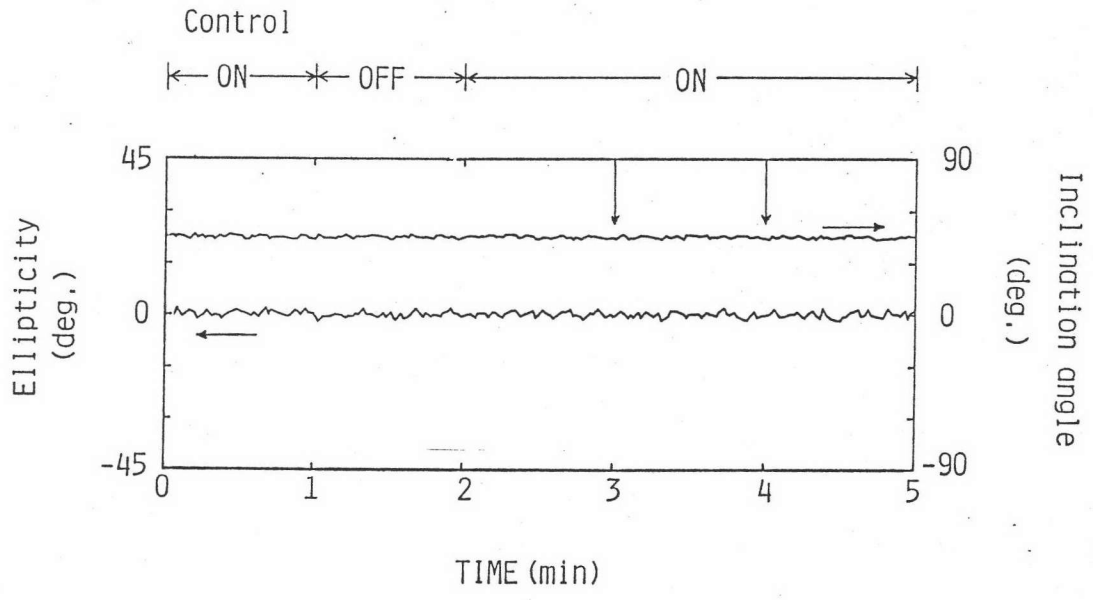

(b)

Fig. 51. Example of results of the polarization-state control experiment utilizing Type-II polarization recombining scheme. The vertical arrows indicate the times when the SOP of the light in the fiber was disturbed.

in about 2.5 sec. (10 steps). A high visibility of 0.94 which corresponds to a 15-dB extinction ratio (10log (P2/P1)) was obtained, whereas the current fluctuation was less than 1%.

Figure 51(b) shows the SOP of the interfering light which has been measured by using a polarimeter located in the place of P1. It is found that the linear SOP with a fixed inclination angle (45° in this case) is preserved regardless of changes in the SOP of the input light.

6.3.3. System experiment

6.3.3.1. Theory:

Schematic diagrams of a diversity receiver system configuration and experimental setup are shown in Fig. 52 and Fig. 53., respectively. In this section analysis on signal-to-noise ratio (S/N) of the system in Fig. 53 is given assuming shot-noise-limited operation.

The electric field of the recombined signals at branch 1 and 2, and the LO: $E_s^{①}$, $E_s^{②}$, and E_{LO} , can be expressed as

$$E_s^{①} = \frac{1}{\sqrt{2}}E_h + \frac{1}{\sqrt{2}}E_v\begin{bmatrix}1\\1\end{bmatrix} \tag{84}$$

$$E_s^{②} = \frac{1}{\sqrt{2}}E_h - \frac{1}{\sqrt{2}}E_v\begin{bmatrix}1\\1\end{bmatrix} \tag{85}$$

$$E_L = \frac{1}{\sqrt{2}}\sqrt{P_L}\exp\{j\phi_L(t)\}\begin{bmatrix} 1 \\ \exp(j\gamma) \end{bmatrix}^T \quad (86)$$

where E_h and E_v denote the electric fields of H: and V: components of the siganl light which can be expressed as

$$E_h = \sqrt{kP_s}\exp\{j[\phi_s(t) + \psi(t) + \theta_h]\} \quad (87)$$

and

$$E_v = \sqrt{(1-k)P_s}\exp\{j[\phi_s(t) + \psi(t) + \theta_v + 2\alpha]\} \quad (88)$$

K denotes the power-splitting factor of the Wollaston prism, P_s and $\phi_s(t)$denote the received signal power and phase, respectively, P_L and $\phi_L(t)$ denote the LO power and phase, respectively, θ_h and θ_v represent the phase of the two respective orthogonal components, $\psi(t)$(= 0 or) is the PSK phase signal, α is the rotation angle of the HWP in the endless phase shifter, and $[\quad]^T$ denote transformation in which the phase shift γ between the orthogonal components of the LO (circularly polarized) light is 90°.

At the monitor branch 2, the photocurrent can be written as

$$\begin{aligned} I_{mon} &= R\left|E_s^{②}.E_s^{②*}\right| \\ &= \frac{1}{2}R[kP_s + (1-k)P_s - 2P_s\sqrt{k(1-k)}\cos\theta_{hv}] \\ &= \frac{1}{2}RP_s[1 - 2\sqrt{k(1-k)}\cos\theta_{hv}] \end{aligned} \quad (89)$$

where the phase term $\theta_{hv} = \theta_h - \theta_v - 2\alpha$ is the phase difference between the two arms of the interferometer. The quatity $R = \eta e/h\nu$ represent the detector responsivity, where η is the quantum efficiency of the photodetector, h is Planck's constant, ν is the velocity of the light, and e is the electron charge.

Next we consider the signals at the receiver branch 1. Assuming that the coupling coefficient of the half-mirrors (HM) is polarization independent and equal to 1/2. Then the output beat signals at branch 3 and 4, respectively, are

$$E_3 = \frac{1}{\sqrt{2}}E_s^{(1)} + \frac{1}{\sqrt{2}}E_L$$

$$= 0.5\left[\begin{array}{l} \sqrt{kP_s}\exp\{j[\phi_s(t) + \psi(t) + \theta_h]\} \\ + \sqrt{(1-k)P_s}\exp\{j[\phi_s(t) + \psi(t) + \theta_v + 2\alpha]\} \\ + \sqrt{P_L}\exp\{j\phi_L(t)\} - x \\ \sqrt{kP_s}\exp\{j[\phi_s(t) + \psi(t) + \theta_h]\} \\ + \sqrt{(1-k)P_s}\exp\{j[\phi_s(t) + \psi(t) + \theta_v + 2\alpha]\} \\ + \sqrt{P_L}\exp\{j[\phi_L(t) + 90°]\} - y \end{array}\right] \quad (90)$$

$$E_4 = \frac{1}{\sqrt{2}}E_s^{(1)} - \frac{1}{\sqrt{2}}E_L$$

$$= 0.5\left[\begin{array}{l} \sqrt{kP_s}\exp\{j[\phi_s(t) + \psi(t) + \theta_h]\} \\ + \sqrt{(1-k)P_s}\exp\{j[\phi_s(t) + \psi(t) + \theta_v + 2\alpha]\} \\ - \sqrt{P_L}\exp\{j\phi_L(t)\} - x \\ \sqrt{kP_s}\exp\{j[\phi_s(t) + \psi(t) + \theta_h]\} \\ + \sqrt{(1-k)P_s}\exp\{j[\phi_s(t) + \psi(t) + \theta_v + 2\alpha]\} \\ - \sqrt{P_L}\exp\{j[\phi_L(t) + 90°]\} - y \end{array}\right] \quad (91)$$

The two orthogonal polarization (H: and V:) components of the two beat signals in eq.(90) and eq.(91) are then separated by the Wollaston prism (WP2 and WP3), and the resulting in-phase (I) and quadrature (Q) signals are subsequently detected by the four photodetectors. The four photocurrents are

$$
\begin{aligned}
I_1 &= R\left|E_3 \cdot E_3^*\right|_x \\
&= 0.25R[kP_s + (1-k)P_s + P_L \\
&\quad + 2P_s\sqrt{k(1-k)}\cos\theta_{hv} \\
&\quad + 2\sqrt{kP_sP_L}\cos(\phi_{sL}(t) + \psi(t) + \theta_h) \\
&\quad + 2\sqrt{(1-k)P_sP_L}\cos(\phi_{sL}(t) + \psi(t) + \theta_v + 2\alpha)] \\
&\quad + n_1(t)
\end{aligned}
\tag{92}
$$

$$
\begin{aligned}
I_2 &= R\left|E_3 \cdot E_3^*\right|_y \\
&= 0.25R[kP_s + (1-k)P_s + P_L \\
&\quad + 2P_s\sqrt{k(1-k)}\cos\theta_{hv} \\
&\quad + 2\sqrt{kP_sP_L}\sin(\phi_{sL}(t) + \psi(t) + \theta_h) \\
&\quad + 2\sqrt{(1-k)P_sP_L}\sin(\phi_{sL}(t) + \psi(t) + \theta_v + 2\alpha)] \\
&\quad + n_2(t)
\end{aligned}
\tag{93}
$$

$$I_3 = R\left|E_4 \cdot E_4^*\right|_x$$

$$= 0.25R[kP_s + (1-k)P_s + P_L + 2P_s\sqrt{k(1-k)}\cos\theta_{hv} - 2\sqrt{kP_sP_L}\cos(\phi_{sL}(t) + \psi(t) + \theta_h) - 2\sqrt{(1-k)P_sP_L}\cos(\phi_{sL}(t) + \psi(t) + \theta_v + 2\alpha)] + n_3(t) \quad (94)$$

$$I_4 = R\left|E_4 \cdot E_4^*\right|_y$$

$$= 0.25R[kP_s + (1-k)P_s + P_L + 2P_s\sqrt{k(1-k)}\cos\theta_{hv} - 2\sqrt{kP_sP_L}\sin(\phi_{sL}(t) + \psi(t) + \theta_h) - 2\sqrt{(1-k)P_sP_L}\sin(\phi_{sL}(t) + \psi(t) + \theta_v + 2\alpha)] + n_4(t) \quad (95)$$

where $\theta_{hv} = \theta_h - \theta_v - 2\alpha$, and $\phi_{sL}(t) = \phi_s(t) - \phi_L(t)$ is the phase noise, and $n_i(t)$ $(i = 1,2,3,4)$ denote noise currents.

We further assume that the four photodetectors are identical, $P_L >> P_s$, and the shot-noise-limited condition is achieved. The output currents of the two balanced recevers are

$$I_x = I_1 - I_3$$

$$= R[\sqrt{kP_sP_L}\cos(\phi_{sL}(t) + \psi(t) + \theta_h) + \sqrt{(1-k)P_sP_L}\cos(\phi_{sL}(t) + \psi(t) + \theta_v + 2\alpha)] + n_x(t) \quad (96)$$

and

$$I_y = I_2 - I_4$$
$$= R[\sqrt{kP_sP_L}\sin(\phi_{sL}(t) + \psi(t) + \theta_h) + \sqrt{(1-k)P_sP_L}\sin(\phi_{sL}(t) + \psi(t) + \theta_v + 2\alpha)] + n_y(t) \quad (97)$$

The variables $n_x(t)$ and $n_y(t)$ denote shot-noise currents having Gaussian probability distribution with a variance σ^2.

$$\langle n_x^2(t)\rangle = \langle n_y^2(t)\rangle = 2\sigma^2 \quad (98)$$

and σ^2 given as [8]

$$\sigma^2 = eRP_LB \quad (99)$$

where B is the reciever bandwith.

The required baseband signals are obtained using one bit delay line (T = bit period) demodulators. We can assume that $\theta_h(t) = \theta_h(t-T)$ and $\theta_v(t) = \theta_v(t-T)$ because the SOP of the signal light drifts slowly [31]. Thus, the baseband signals can be expressed as

$$V_x = r[I_x(t).I_x(t-T)]$$
$$= R^2r[\frac{k}{2}P_sP_L\cos(\Delta\phi + \Delta\psi) + \frac{1}{2}(1-k)P_sP_L\cos(\Delta\phi + \Delta\psi) + P_sP_L\sqrt{k(1-k)}\cos(\Delta\phi + \Delta\psi)\cos\theta_{hv} + \sqrt{kP_sP_L}\cos(\phi_{sL}(t) + \psi(t) + \theta_h)n_x(t-T) + \sqrt{(1-k)P_sP_L}\cos(\phi_{sL}(t) + \psi(t) + \theta_v + 2\alpha)n_x(t-T) + \sqrt{kP_sP_L}\cos(\phi_{sL}(t-T) + \psi(t-T) + \theta_h)n_x(t) + \sqrt{(1-k)P_sP_L}\cos(\phi_{sL}(t-T) + \psi(t-T) + \theta_v + 2\alpha)n_x(t) + n_x(t)n_x(t-T)] \quad (100)$$

$$
\begin{aligned}
V_y &= r[I_y(t).I_y(t-T)] \\
&= R^2 r[\frac{k}{2}P_s P_L \cos(\Delta\phi + \Delta\psi) + \frac{1}{2}(1-k)P_s P_L \cos(\Delta\phi + \Delta\psi) \\
&\quad + P_s P_L \sqrt{k(1-k)}\, \cos(\Delta\phi + \Delta\psi)\cos\theta_{hv} \\
&\quad + \sqrt{kP_s P_L}\, \cos(\phi_{sL}(t) + \psi(t) + \theta_h)n_y(t-T) \\
&\quad + \sqrt{(1-k)P_s P_L}\, \cos(\phi_{sL}(t) + \psi(t) + \theta_v + 2\alpha)n_y(t-T) \\
&\quad + \sqrt{kP_s P_L}\, \cos(\phi_{sL}(t-T) + \psi(t-T) + \theta_h)n_y(t) \\
&\quad + \sqrt{(1-k)P_s P_L}\, \cos(\phi_{sL}(t-T) + \psi(t-T) + \theta_v + 2\alpha)n_y(t) \\
&\quad + n_y(t)n_y(t-T)]
\end{aligned}
\tag{101}
$$

where r is a constant, $\Delta\phi = \phi_{sL}(t) - \phi_{sL}(t-T)$ is the phase noise and $\Delta\psi = \psi(t) = \psi(t-T)$.

Hence, the sum of the two signal yields the total basband signal,

$$V = \pm rR^2 P_s P_L \cos\Delta\phi[1 + 2\sqrt{k(1-k)}\cos\theta_{hv}] \tag{102}$$

which depends on the phase noise $\Delta\phi$, and the SOP of the received signal (i.e. the power-splitting factor of the Wollaston prism k and phase difference between the two orthogonal components of the signal light θ_{hv}. The upper plus sign corresponds to the mark signal and the lower minus sign corresponds to the space signal.

Since we are interested only in the effect of the polarization fluctuation, so the phase noise is ignored (i.e. $\Delta\phi = 0$). For simplicity, the polarization phase difference θ_{hv} is assumed to be constant over a bit

period. Under this condition the mean value of the baseband signal is given by

$$E[V] = \pm rR^2 P_S P_L [1 + 2\sqrt{K(1-k)}\cos\theta_{hv}] \quad (103)$$

As the Gaussian noise terms have zero mean value, all the cross-product terms involving noise voltage terms $n_x(t)$, $n_y(t)$, $n_x(t-T)$, and $n_y(t-T)$ in eq.(100) and eq. (101) also have zero mean. Thus, the variance of the signal is given by

$$\begin{aligned} Var[V] &= E[V^2] - E[V]^2 \\ &= 8r^2(R^2 P_S P_L \sigma^2 + \sigma^4) \end{aligned} \quad (104)$$

Hence, the S/N under the shot-noise-limited operation can be expressed as

$$\begin{aligned} S/N &= \frac{E[V]^2}{Var[V]} \\ &= \frac{r^2 R^4 P_s^2 P_L^2 [1 + 2\sqrt{k(1-k)}\cos\theta_{hv}]^2}{8r^2(R^3 P_s P_L^2 eB + e^2 R^2 P_L^2 B^2)} \\ &= \frac{RP_s[1 + 2\sqrt{k(1-k)}\cos\theta_{hv}]^2}{8eB} \end{aligned} \quad (105)$$

In an ideal polarization aligned DPSK heterodyne receiver operating under the shot-noise-limited condition [8], the S/N is given

$$(S/N)_i = RP_S/2eB \quad (106)$$

According to eq.(105), when k = 0.5, and $\theta_{hv} = 2m\pi$ (m:interger), the optimum S/N equal to eq.(106) is

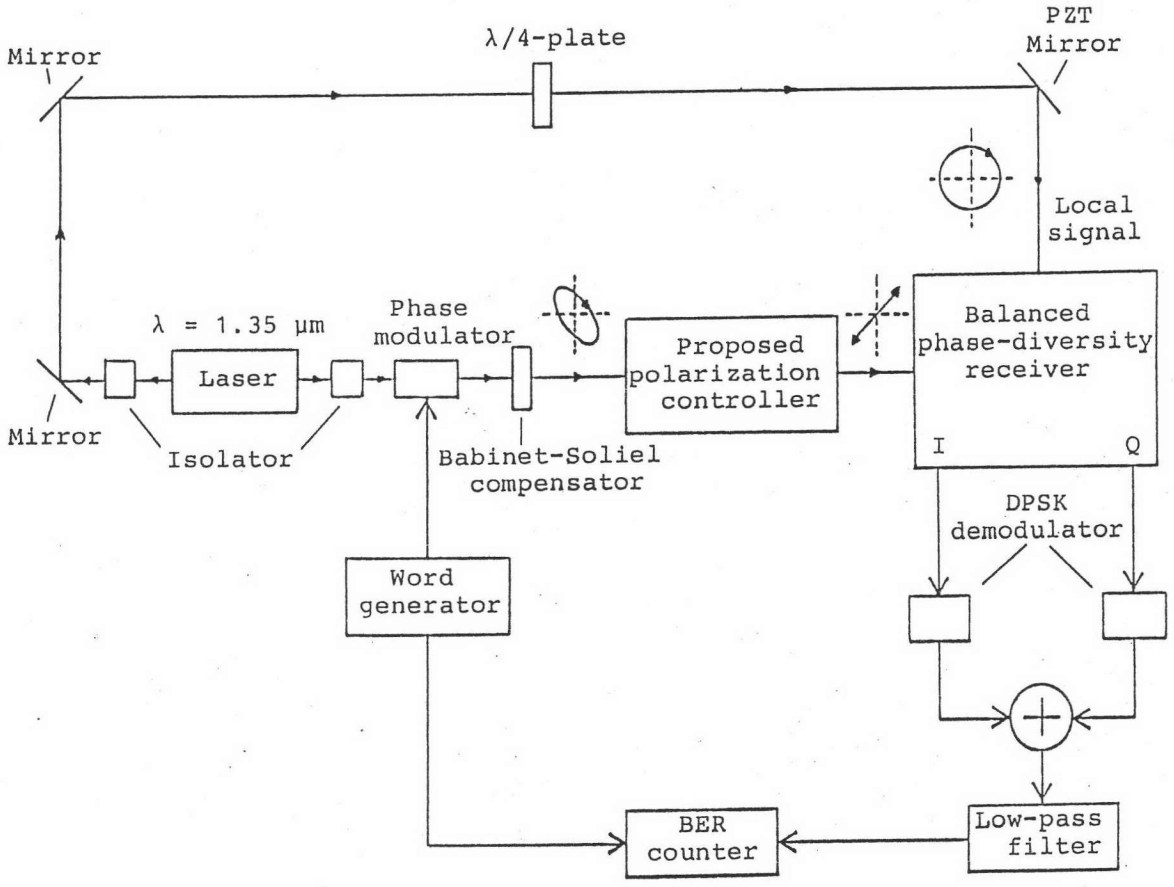

Fig. 52. System configuration of a self-homodyne balanced phase diversity receiver with automatic polarization-state control.

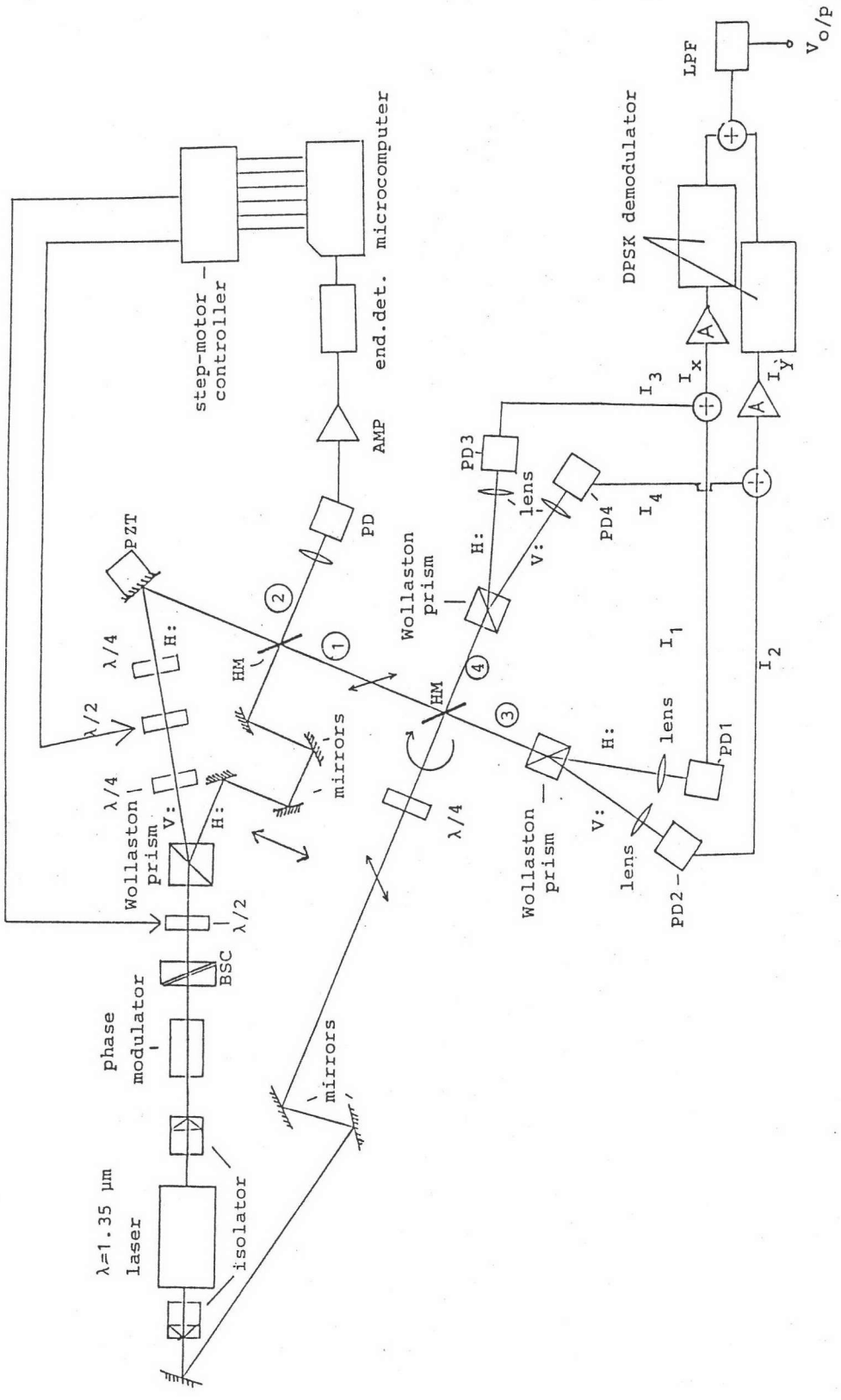

Fig. 53. Experimental setup of automatic polarization-state control for 200 Mb/s DPSK self-homodyne balanced phase diversity receiver.

achieved. This is the operating condition of the proposed SOP control scheme (i.e. when the monitor current is zero (in eq.(89), $I_{mon} = 0$)).

In the worst case there will be no signal power at branch 1 when k = 0.5, and $\theta_{hv} = m\pi$ (m = 1, 3, 5,...). This time all the signal power contributes to the monitor branch 2 ($I_{mon} \cong P_s$).

When k = 0 or 1, or $\theta_{hv} = m\pi/2$ (m = 1, 3, 5,...), the S/N is degraded by 6 dB. as compared with the ideal case. The reason is that half of the signal power is lost to the monitor branch ($I_{mon} \cong P_s/2$).

The S/N degradation is given by

$$(S/N)_{deg} = \frac{(S/N)_i}{S/N} = \frac{[1 + 2\sqrt{k(1-k)}\cos\theta_{hv}]^2}{4} \qquad (107)$$

Figure 54 shows the plots of S/N degradation as a function of k for different values of θ_{hv}.

6.3.3.2. Experiment and results

The experimental set-up which simulates a phase diversity optical homodyne receiver, is shown in Fig. 53. A self-homodyne detection was chosen because we were only interested in the impact of the polarization fluctuation of the signal light. This eliminated the effects of the laser phase noise and the IF frequency fluctuation. The two output beams of a 1.35 μm DFB laser were utilized. One was used as the LO light whose

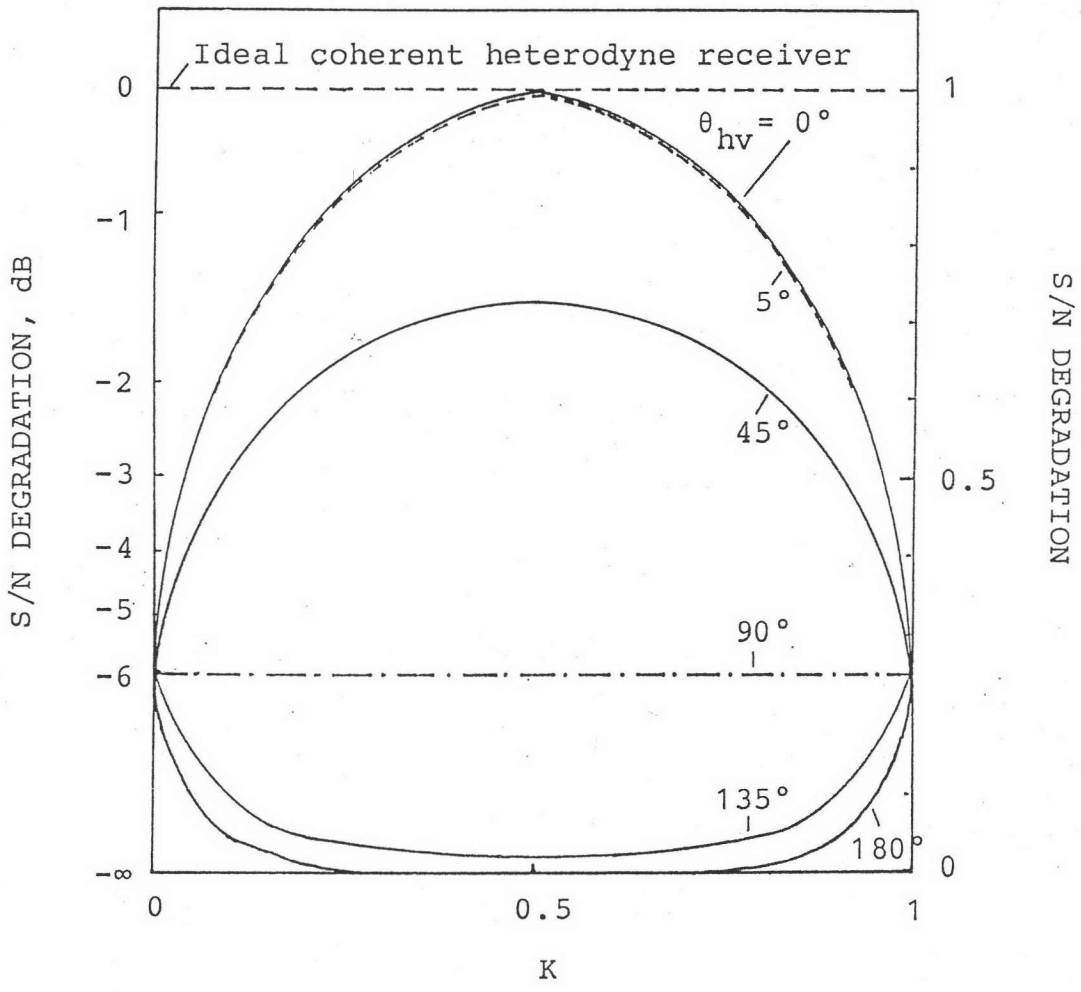

Fig. 54. S/N degradation as a function of power-splitting factor of a polarization-beam splitter for the phase difference θ_{hv} = 0°, 5°, 45°, 90°, 135°, and 180°.

SOP was transformed into to a circular polarization by the QWP. The second beam (regarded as the signal) was phase-modulated by a 200 Mbits/s fixed pattern using a $LiTaO_3$ phase modulator, and passed through the BSC and then through the polarization controller. Two beams were mixed in a balanced 90° optical hybrid configuration [64] which generated two pairs of 180°-out-of-phase beat signals. One pair was regarded as in-phase (I) signal and the other was quadrature (Q) one. Each pair was homodyne-detected seperately by two similar balanced receievers, each of which consisted of two Ge-APD photodetectors balanced between opposite polarity bias supplies [102]. The bias voltages were kept low (5V) in order to suppress the detectors' excess noise. The resulting balanced I and Q signals were amplified and then connected to the standard DPSK delay demodulators followed by an electrical combiner, a low pass filter, and a bit-error-rate (BER) counter.

The polarization control system configuration in this experiment was almost identical to the one used in Fig. 50. The differences were that the FC1 was replaced by the BSC and the FC2 was replaced by a rotatable HWP (not shown in Fig. 53).

To demonstrate the polarization-insensitibility of the 90 optical hybrid against changes in SOP of the signal light at the polarization controller input, the unmodulated I and Q signals were, respectively, fed to

the x and y input terminals of an oscilloscope. By piezoelectrically moving a mirror (with a 100 Hz. sawtooth waveform) which was located in the LO path, as a result, a circular Lissajous pattern was generated and displayed on the oscilloscope screen. An example of the results was shown by the photographs in Photo. 3. These photographs indicate that the AC-terms of the I and Q signals were in quadrature regardless of change in the signal SOP, only the magnitudes that were effected. In Photo. 4, the 45°-inclined linear polarization-state of the signal light has been confirmed. Note that this experiment was performed when the polarization control was switched off and the polarization disturbance was given by the BSC.

Figure 55 shows the system performance with and without polarization control. BER around 10^{-6} was chosen in order to reduce the BER measurement time. During the measurements, the SOP of the signal light was intentionally disturbed by manipulating the BSC at T= 70, 140, 220, and 270 s. It is found that BER was kept stable within two order of magnitudes which corresponded to receiver sensitivity fluctuation of 0.5 dB, under the polarization control. With the polarization control off, the BER was significantly deterioated as the signal SOP was varried, which resulted in a sensitivity degradation of more than 5 dB in this experiment. The measured LO power at the input of the 90° optical hybrid was -9.2 dBm, and that of the signal

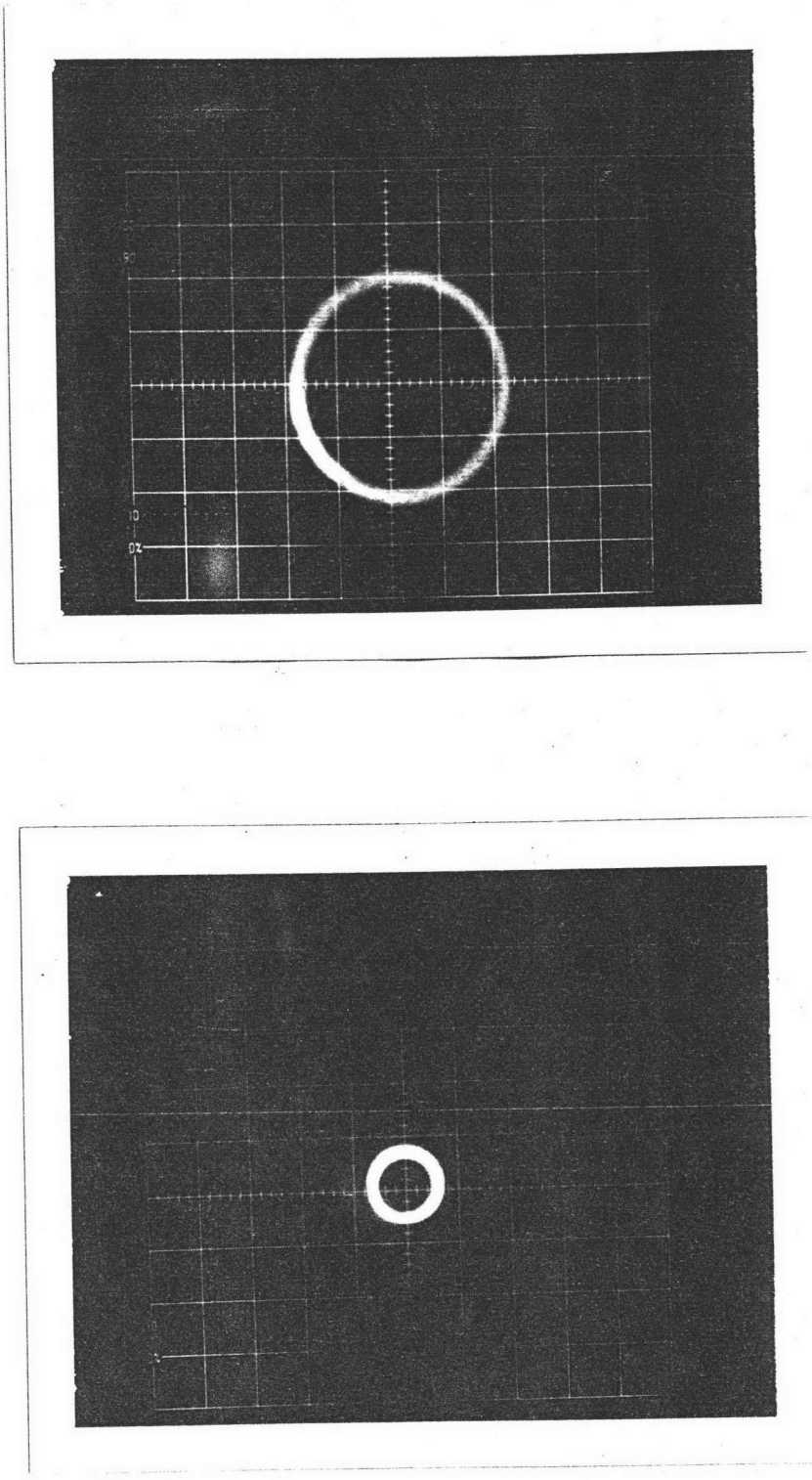

Photo. 3. Lissajous patterns obtained with two orthogonal (I and Q) beat signals. (scale: 20mV/div)

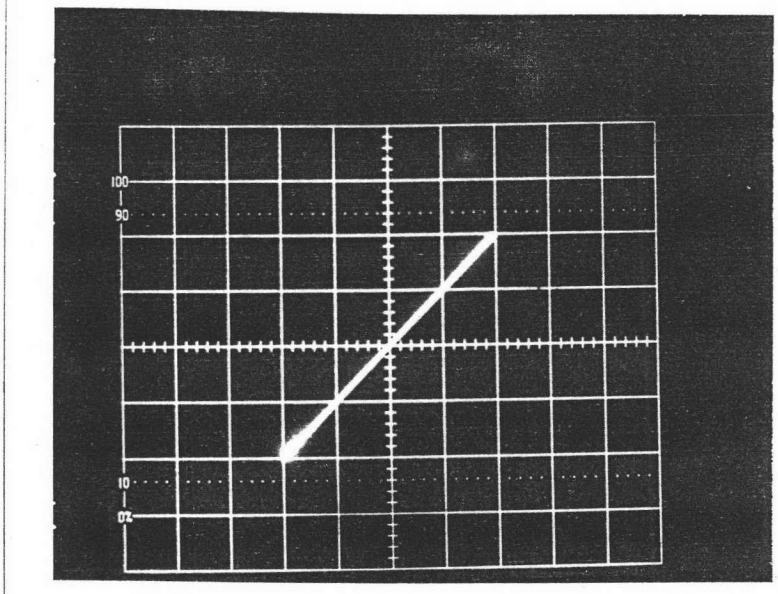

(a)

change in SOP

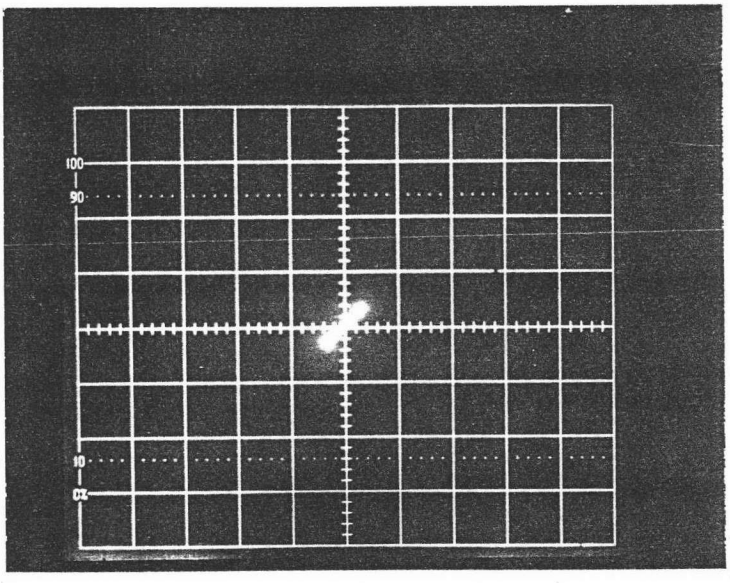

(b)

Photo. 4. X - Y plot of the polarization recombined signals only, (i.e. $P_L = 0$). (scale: 20 mV/div)

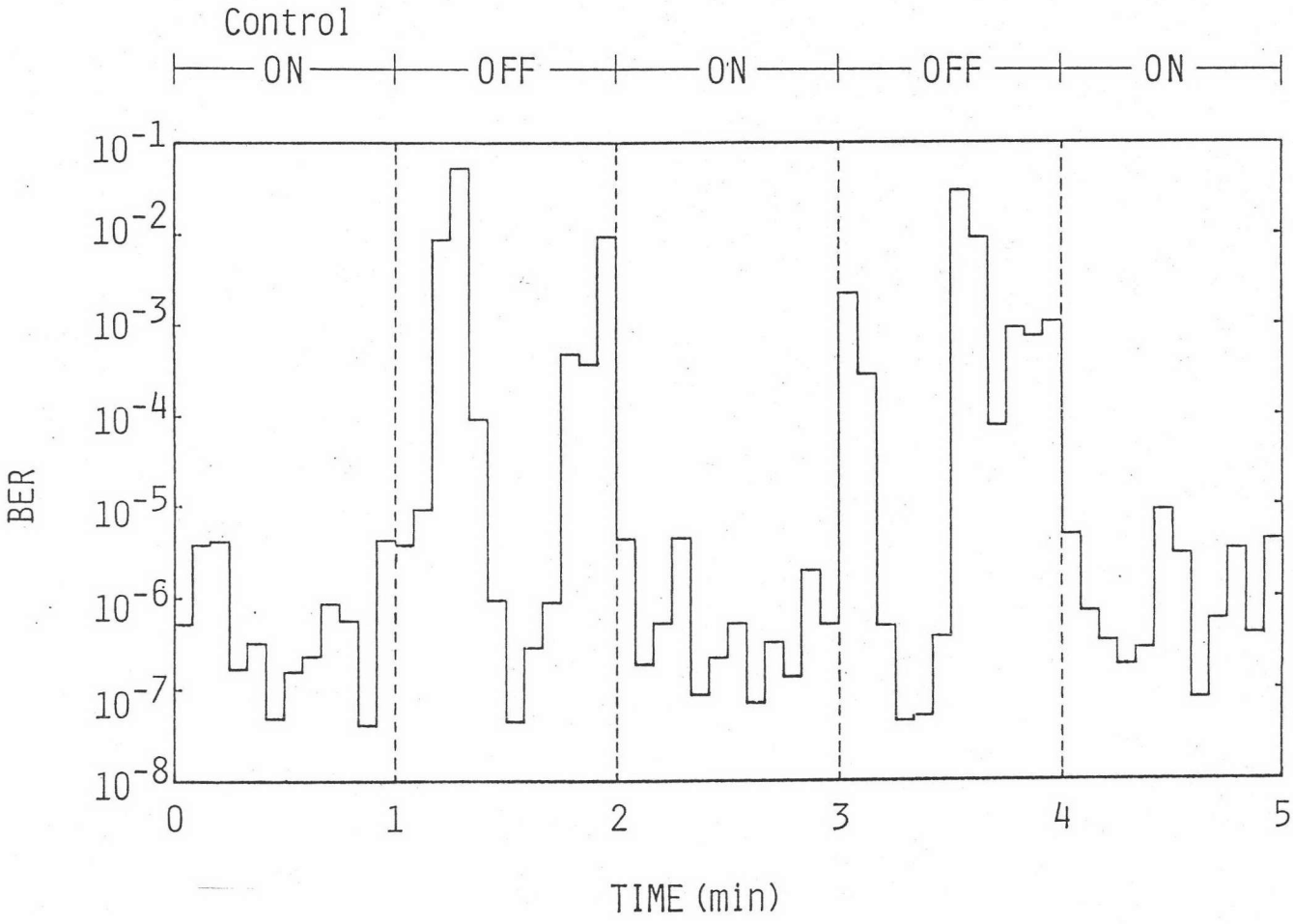

Fig. 55. System performance with polarization control on and off. (BER was measured every 5 s., so 60 readings were taken during 5 min.).

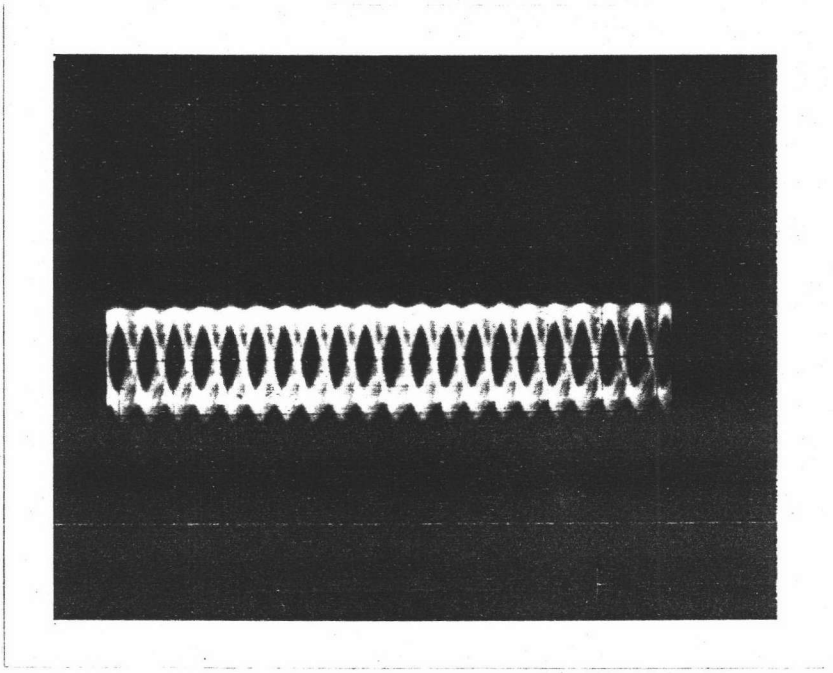

Photo. 5. Eyepattern for 200 Mb/s DPSK fixed pattern. (H: 10 msec/div)

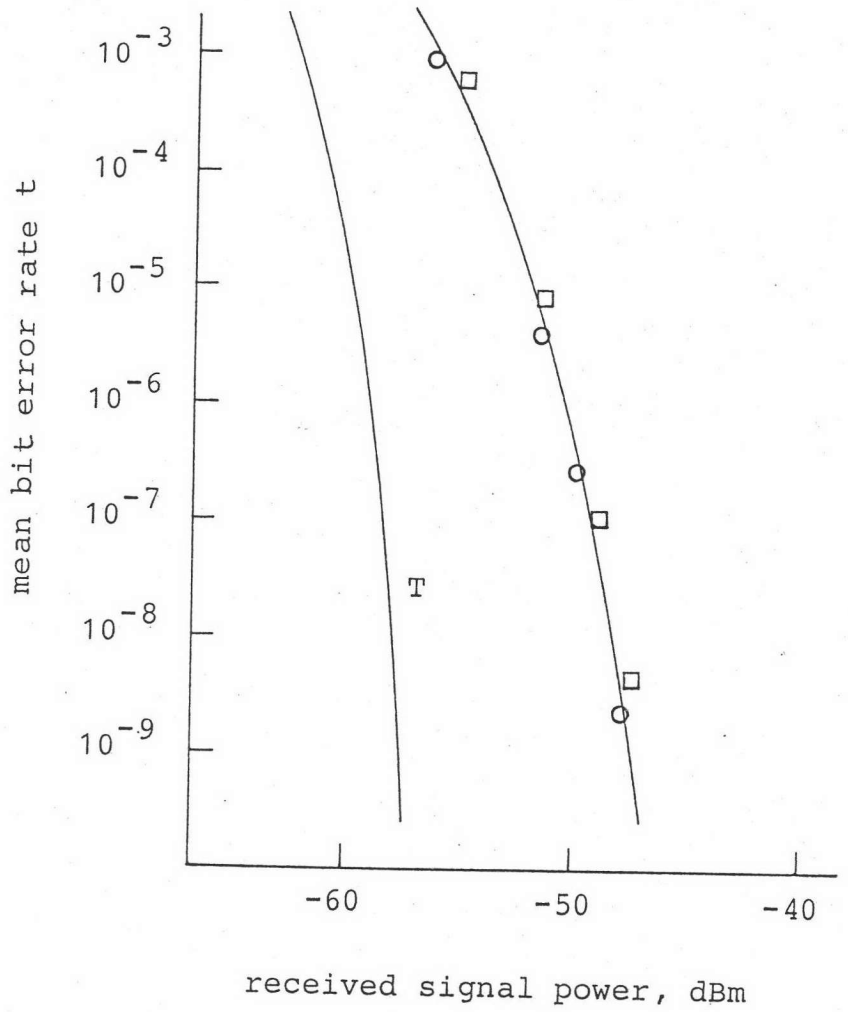

Fig. 56. Bit error rate against received signal power.
Theory :shot-noise-limited performance - (T) (after Okoshi [8]);
Measured : polarization aligned (conventional) phase diversity receiver - (O); automatic polarization control phase diversity receiver - (□).

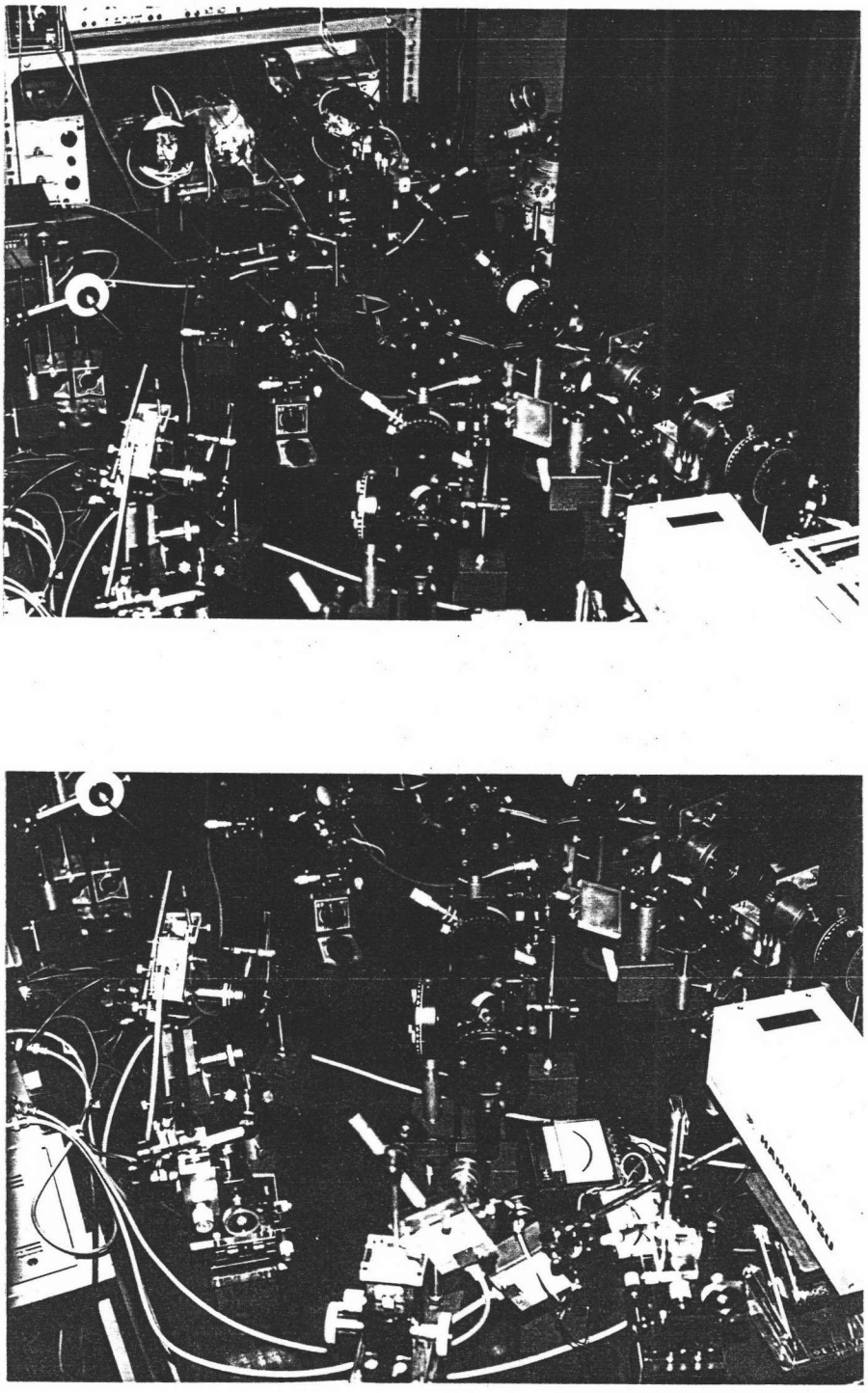

Photo. 6. Experimental setup for a self-homodyne balanced phase diversity receiver.

was -41.7 dBm at maximum level.

Figure 56 compares the BER performance of the present system with that of the polarization aligned system. In the latter system, the polarization controller was removed and the correct SOP of the signal light was obtained by using a polarizer. The rest of the system was the same as before. The 0.5 dB penalty, measured at BER of 10^{-8} for the polarization controlled receiver as compared with the polarization aligned receiver, was mainly due to the signal power loss caused by the insertion loss of the polarization control system. And about 10 dB degradation of both receivers from the theory was caused in part by the excess noise of the Ge-APD photodetectors, insufficient LO power, unbalanced receivers, amplifiers noise, imperfect modulation, and other instabilities. Note that the theoretical curve in Fig. 56 is calculated from the shot-noise-limitd DPSK heterodyne receiver sensitivity given by eq.(38) in [8], since the receiver sensitivity for DPSK phase diversity is the same as that for conventional DPSK heterodyne receiver [27].

6.4. Summary

Two types of SOP control schemes using polarization recombing technique have been verified experimentally. The endless in control is achieved by mechanical control which can maintain the signal stability

within 1% of the average value. Feasibility of the SOP control in phase diversity receiver has also been demonstrated employing a self-homodyne DPSK system. And the fluctuation of the receiver sensitivity is found to be within the range of 0.5 dB at 200 Mbits/s.